

A cluster-induced structural disorder and melting transition in the grain boundary of B2 NiAl: a molecular-dynamics simulation on parallel computers

This article has been downloaded from IOPscience. Please scroll down to see the full text article.

2000 J. Phys.: Condens. Matter 12 L549

(<http://iopscience.iop.org/0953-8984/12/34/102>)

View [the table of contents for this issue](#), or go to the [journal homepage](#) for more

Download details:

IP Address: 171.66.16.221

The article was downloaded on 16/05/2010 at 06:40

Please note that [terms and conditions apply](#).

## LETTER TO THE EDITOR

**A cluster-induced structural disorder and melting transition in the grain boundary of B2 NiAl: a molecular-dynamics simulation on parallel computers**S J Zhao<sup>†</sup>, S Q Wang<sup>†</sup>, T G Zhang<sup>‡</sup> and H Q Ye<sup>†</sup><sup>†</sup> Laboratory of Atomic Imaging of Solids, Institute of Metal Research, Chinese Academy of Sciences, Shenyang 110015, People's Republic of China<sup>‡</sup> Institute of Jiang Nan Computer Technology, Wuxi 214083, People's Republic of China

E-mail: sjzhao@imr.ac.cn

Received 1 August 2000

**Abstract.** A structural disorder and melting transition of the  $\Sigma = 5$  bicrystalline interface of B2 NiAl with a large boundary plane is investigated by molecular-dynamics simulations. The calculations have been performed at various temperatures using an embedded-atom-method potential fitted to NiAl. It is observed that the atoms in the grain-boundary region tend to form clusters in a thermal structural disorder transition, which is initiated at a temperature well below the thermodynamic melting point  $T_m$  (around  $0.52T_m$ ). The number and size of the clusters are monitored over a wide temperature range including  $T_m$ . Below  $T_m$ , the number and size of the clusters increase continuously with increasing temperature. At temperatures up to  $T_m$ , the abrupt increase in size of the clusters induces melting. At temperatures above  $T_m$ , the number and size of the clusters decrease significantly upon raising temperature. The calculations of the potential energy also indicate that the thermal disorder transition is a continuous process, in contrast to the first-order melting transformation.

Experiments cannot give us detailed information on the atomic-level behaviour of the boundary structure at elevated temperatures since direct observations are extremely difficult. Molecular-dynamics (MD) simulations are effective to investigate the atomic structure at the interface over a temperature range up to the melting point of the crystal [1–6]. A disorder and melting transition was found to initiate at the interface in the simulations, and was called a lattice-defect-nucleated process [4–6]. However, due to limitations in computational resources and speed, the boundary plane is conventionally chosen to be relatively small [1–6], and more detailed information about such a lattice-defect-nucleated process cannot be provided due to the small boundary plane. For example, a recent experiment [7] indicated that the melting was strongly influenced by the size of clusters. The formation and disappearance, and the growth and collapse of clusters in the grain-boundary (GB) region play an important role in the order-to-disorder and solid-to-liquid transitions at elevated temperatures [8]. If the boundary plane is not chosen large enough, the emergence of sub-critical clusters (known as embryos) cannot be observed at all in simulations.

In this work, with the help of parallel computing and the rapid increase in computing speed, a large system with a large boundary plane is simulated by the MD method. The large size of the boundary plane ensures not only the emergence of clusters, but also meaningful statistics when computing the number and size of those clusters. All the simulations are performed for constant number ( $N$ ), constant volume ( $V$ ) and constant temperature ( $T$ ) by using the damped

force method [9]. Our calculations indicate that the thermal structural disorder transition is a continuous process, in contrast to the first-order melting transformation.

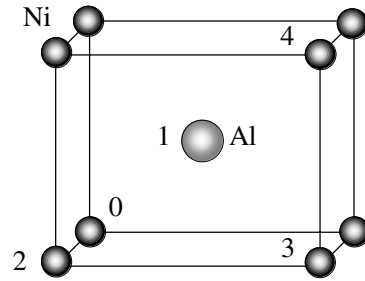


**Figure 1.** The B2 crystal structure of NiAl, with nearest neighbour (NN) distance  $0.866a$ , second NN  $a$ , third NN  $1.414a$ , fourth NN  $1.732a$ , and so on.

Figure 1 shows the B2 crystal structure of NiAl and its relationship with neighbouring atoms. There are two models in our simulation work: cell A representing a single perfect crystal with three-dimensional (3D) periodic-border conditions, and cell B representing a bicrystal in the presence of a  $\Sigma = 5$   $36.86^\circ$  (310)/[001] GB with 219 816 atoms, analogous to the bicrystal model of Lutsko *et al* [10]. Cell B was divided into 64 independent units, which were calculated independently and simultaneously by using 64 processing elements (PE) on parallel computers. The parallel computing was implemented by using a message passing interface (MPI) technique. Cell A is a perfect B2 lattice with six unit cells along each direction,  $6a * 6a * 6a$ , containing 432 atoms in all. All the particles interact via an embedded-atom-method (EAM) potential empirically fitted to B2 NiAl [11].

In addition to the potential energy per atom (PEPA)  $U$ , the static structure factor  $S$ , which is defined as

$$S = \frac{1}{N^2} \left| \sum_i \exp(i\mathbf{k} \cdot \mathbf{r}_i) \right|^2 \quad (1)$$

was calculated during the simulations. In the above expression,  $r_i$  represents the position of atom  $i$  and  $N$  is the number of atoms considered.  $\mathbf{k}$  is a prescribed wavevector which is a reciprocal-space vector of the B2 structure. In this work,  $\mathbf{k}$  is chosen along the [001] direction,  $\mathbf{k} = (0, 0, 4\pi/a)$ . For an ideal-crystal lattice at zero temperature  $S$  equals unity. By contrast, in a liquid state,  $S$  fluctuates near zero due to the absence of long-range order.

We first consider the reference-bulk results based on the simulations using cell A. The simulations are performed over a wide temperature range from  $0.15T_m$  to  $1.47T_m$ . The temperature dependence of the PEPA  $U$  is shown in figure 2 (see the open circles). The profile shows that the potential energy increases linearly with temperature up to  $1.30T_m$ . At  $1.32T_m$ , the energy increases to a distinctly higher value,  $-3.814$ , while  $S$  decreases to 0.009 (we note that  $S = 0.842$  at  $1.30T_m$ ) almost instantaneously, which is typical of a liquid phase. It is demonstrated that the crystalline lattice has collapsed at  $1.32T_m$ , and the temperature  $1.32T_m$  is the mechanical melting point  $T_s$  [4, 5] corresponding to the current system. The difference between the mechanical melting point  $T_s$  and the thermodynamic melting point  $T_m$  is the range in which the model solid can be superheated.

We have also carried out simulations at various temperatures ranging from  $0.15T_m$  to  $1.22T_m$ . The lattice constant  $a$  is chosen to be the experimental value at the corresponding temperature. The temperature dependence of the structural local properties in the GB region is investigated by computing the total pair distribution function ( $g(r_{tot})$ ) and the partial pair

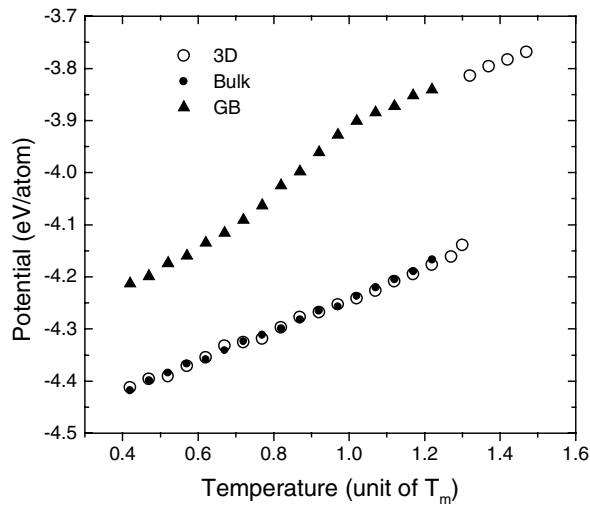


**Figure 2.** Temperature variation of potential energy per atom in the grain boundary (full triangles). Also shown are potential energy values for the bulk region (full circles) and for the 3D-periodic single-crystal cell (open circles).

distribution functions ( $g(r_{NiNi})$ ,  $g(r_{NiAl})$  and  $g(r_{AlAl})$ ). Figure 3 shows the profiles of  $g(r)$  in the GB region at  $0.47T_m$ ,  $0.67T_m$  and  $1.02T_m$ .

At  $0.47T_m$ , the peaks are sharp and well defined, and appear at the correct neighbour distances as shown in figure 1. The profiles show that the structure in the GB region at  $0.47T_m$  is still highly ordered. When the temperature is raised further, the peaks decline quickly and

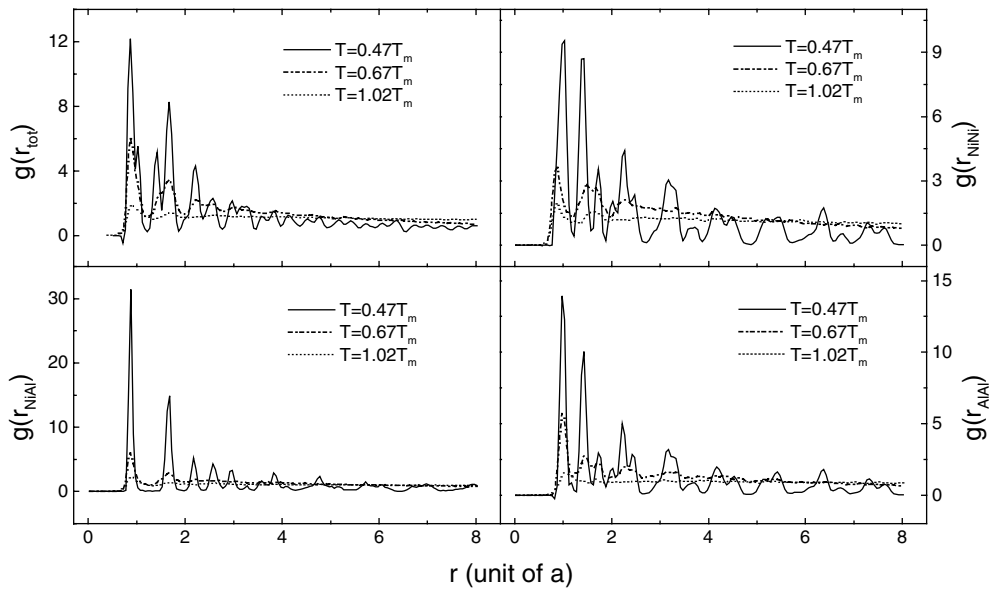


**Figure 3.** Total pair distribution function  $g(r_{tot})$  and partial pair distribution functions  $g(r_{NiNi})$ ,  $g(r_{NiAl})$  and  $g(r_{AlAl})$  at  $0.47T_m$ ,  $0.67T_m$  and  $1.02T_m$ .

there is a loss of resolution (see the temperature variation of the third and fourth peaks in  $g(r_{tot})$ , the second and third peaks in  $g(r_{NiNi})$  and  $g(r_{AlAl})$ ). This can be taken as a qualitative indication of a structural disorder transition in the GB region. When the temperature is raised to  $1.02T_m$ , the peaks become broad and the curves of  $g(r)$  tend to unity, which is typical of a liquid phase.

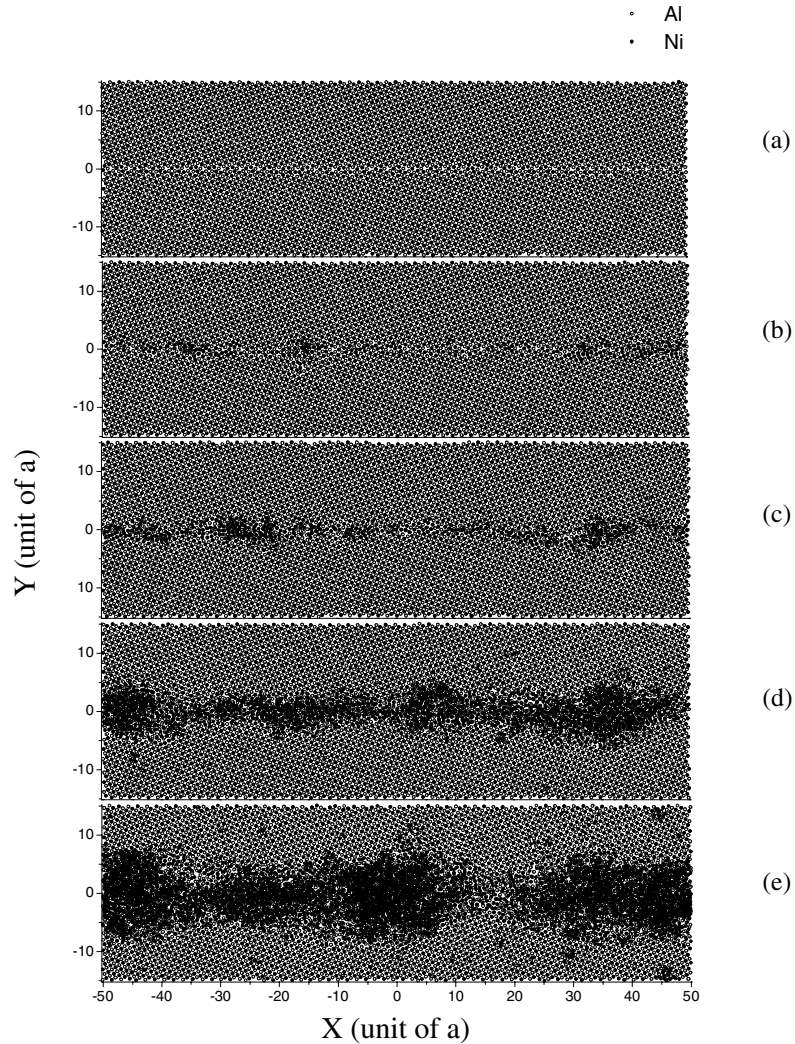


**Figure 4.** Snapshot of the GB atoms, projected onto the  $x$ - $y$  plane, at (a)  $0.47T_m$ , (b)  $0.52T_m$ , (c)  $0.67T_m$ , (d)  $0.97T_m$  and (e)  $1.02T_m$ , respectively. Open circles represent Al atoms and full circles represent Ni atoms.

Figure 4 shows five snapshots of the GB atoms, projected onto the  $x$ - $y$  plane, between  $0.47T_m$  and  $1.02T_m$ . From  $0.15T_m$  to  $0.47T_m$ , an orderly GB region can still be observed. When the temperature is raised further, the atoms in the GB region tend to form groups. Here, we call such atomic groups 'clusters' (or liquid embryos), which are defined as follows: for any given atom  $i$  in a cluster, at least one other atom in the same cluster, whose distance from the atom  $i$  is no more than  $r_{cluster}$ , can always be found. In this work,  $r_{cluster}$  is chosen to be  $0.83a$ .

The size of a cluster can be denoted either by the radius  $r$  or by the number of atoms included in the clusters. Since the shape of the cluster is not a strict sphere, it seems to be more rational to use the number of atoms included. In this work, only the clusters in which the number of atoms included is more than eight are added up. The boundary plane is chosen to be sufficiently large to have meaningful statistics when computing the number and size of those clusters.

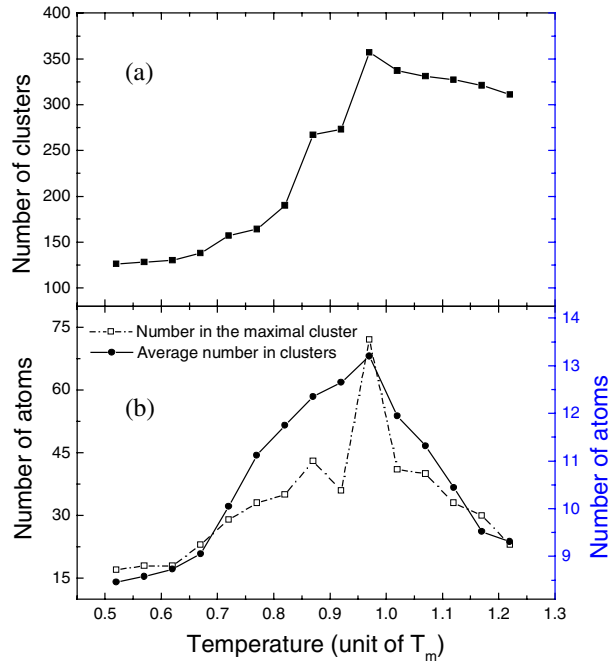


**Figure 5.** Temperature dependence of (a) number of clusters, (b) size of the maximal cluster (left-hand scale) and average size of clusters (right-hand scale).

Figure 5(a) is the profile of the number of clusters against temperature. The number of clusters increases very slowly with increasing temperature up to  $0.62T_m$ , then rises sharply from  $0.67T_m$  to  $0.97T_m$ . This behaviour is reminiscent of the Lindemann criterion for melting, requiring a certain amount of thermal disordering in order to trigger the melting transition [12]. At  $1.02T_m$ , the number of clusters has a decrease, and figure 5(a) shows that the portion of the curve between  $1.02T_m$  and  $1.22T_m$  decreases gradually. It is demonstrated that after the solid-to-liquid phase transition, some clusters have worn away, and the higher the temperature, the fewer the clusters.

Figure 5(b) shows the temperature dependence of the size of the maximal cluster (left-hand scale) and the average size of the clusters (right-hand scale). Similarly to the profile in figure 5(a), the size of the clusters increases slowly upon raising temperature at the beginning, then increases quickly up to  $0.97T_m$ . In contrast, when temperatures are above  $1.02T_m$ , the size of the clusters decreases upon heating. Apparently, after the solid-to-liquid phase transition, the clusters split. Moreover, the higher the temperature, the smaller the clusters.

The number of atoms in the maximal cluster increases very slowly upon raising temperature from  $0.52T_m$  to  $0.62T_m$  and the size of the maximal cluster can be treated as invariant. This shows that at low temperatures smaller clusters begin to form and can lie in the GB region stably. The size of the maximal cluster becomes continuously larger with increasing temperature. Just

before the thermodynamic melting point  $T_m$ , the size of the maximal cluster increases to a distinctly higher value, which is probably caused by the coalescence of many clusters. The abrupt increase in size of the maximal cluster accelerates the solid-to-liquid phase transition. When the temperature rises to  $1.02T_m$ , by contrast, the size of the maximal cluster has an abrupt decrease. All these results indicate that there exists a critical size in the growing of the clusters and after the melting transition the critical-sized cluster has collapsed.

The maximal cluster has a higher proportion of surface atoms, which are more weakly bound and less constrained in their thermal motion [13, 14] than those in bulk. At  $T_m$ , due to a combined effect of thermal fluctuations and an intrinsic elastic instability in the system, the crystalline structure of the critical-sized maximal cluster collapses abruptly and turns heterogeneously into a liquid structure. Then melting propagates into other clusters and into the bulk quickly. For systems without extrinsic defects, melting is an intrinsic process initiated by a spontaneous homogeneous nucleation mechanism. A homogeneous melting can lead to a higher melting point beyond that of the bulk solid (see the above superheating results of the perfect single crystal). However, for systems with extrinsic defects such as GBs, the melting can be referred to as a heterogeneous process. In this work, it is found that the clusters in the GB region act as the heterogeneous nucleation sites for the liquid phase. The variation tendency (i.e., monotonically decreasing upon heating) of the number and size of the clusters above  $T_m$  is apparently contrary to the behaviour (i.e., monotonically increasing upon heating) in the structural disorder transition below  $T_m$ . The disordered structure of GB below  $T_m$  is compatible with a description of the GB as a crystalline solid with short-range ordered cluster concentration, while the structure of the GB above  $T_m$  can be described as a liquid, in which small unstable crystalline clusters are suspended.

The continuously increasing number and size of the clusters indicates that the disordering in the GB region at  $T < T_m$  is a continuous process. The temperature variation of the potential energy can give us a better understanding of this process. Figure 2 also shows the temperature variation of the potential energy  $U$  for the bicrystal model. The open circles and the full circles in figure 2, which represent the perfect single crystal and the bulk of the bicrystal, respectively, are nearly overlapping over a temperature range from  $0.42T_m$  to  $1.22T_m$ . The agreement indicates that the existence of the GB in our system does not prevent the bulk from reaching its thermodynamic equilibrium after the full relaxation in current simulations. The energy of the GB (the full triangles in figure 2) increases linearly with increasing temperature up to  $0.49T_m$ . At  $0.52T_m$ , the GB energy is found to deviate from the straight line, which is ascribed to the beginning of disorder. Then the energy of the GB increases continuously all the way up to  $0.97T_m$ . When temperature reaches  $1.02T_m$ , the energy of the GB falls on a straight-line extrapolation from the liquid branch of the single crystal's curve (see the open circles above  $1.3T_m$  in figure 2). All these results show that this transition is very smooth and the partially disordered structure near the boundary core, initiated at a temperature below  $T_m$ , goes continuously to liquid structure at  $T_m$ .

In summary, parallel MD simulations have been performed to investigate the order-to-disorder and solid-to-liquid transition in the GB region at elevated temperatures. The system tends to form clusters at a temperature well below  $T_m$ . Upon heating, the number and size of the clusters increase up to the thermodynamic melting temperature  $T_m$ . Our results indicate that the order-to-disorder transition in the GB region is a continuous process, which supports the theoretical prediction, i.e., thermal disordering in a crystal interface is a continuous process, in contrast to the first-order melting transformation [15]. Near temperature  $T_m$ , the size of the clusters has an abrupt increase, which promotes the melting process. Once the temperature is above  $T_m$ , the size of the clusters begins to decrease abruptly, which is regarded as evidence that the large clusters have split at  $T_m$ . Moreover, the higher the temperature, the fewer the clusters.

The completely dissimilar behaviour of the clusters between the thermal structural disorder transition and the melting phase transition provides us with a new clue to understanding two such qualitatively different processes.

We thank Professor Wang Yuanming for many useful discussions. This work was supported by National Pandeng Research Project (No 95-Yu-41) and National Natural Science Foundation (No 59831020) of China.

## References

- [1] Kikuchi R and Cahn J W 1980 *Phys. Rev. B* **21** 1893
- [2] Deymier P, Taiwo A and Kalonji G 1987 *Acta Metall.* **35** 2719
- [3] Nguyen T, Ho P S, Kwok T, Nitta C and Yip S 1986 *Phys. Rev. Lett.* **57** 1919
- [4] Phillpot S R, Lutsko J F, Wolf D and Yip S 1989 *Phys. Rev. B* **40** 2831
- [5] Lutsko J F, Wolf D, Phillpot S R and Yip S 1989 *Phys. Rev. B* **40** 2841
- [6] Nguyen T, Ho P S, Kwok T, Nitta C and Yip S 1992 *Phys. Rev. B* **46** 6050
- [7] Schmidt M, Kusche R, Issendorff B V and Haberland H 1998 *Nature* **393** 238
- [8] Koblinski P, Wolf D, Phillpot S R and Gleiter H 1999 *Phil. Mag. A* **79** 2735
- [9] Hoover W G 1983 *Physica A* **118** 111
- [10] Lutsko J F, Wolf D, Yip S, Phillpot S R and Nguyen T 1988 *Phys. Rev. B* **38** 11 572
- [11] Farkas D, Mutasa B, Vailhe C and Ternes K 1995 *Modelling Simul. Mater. Sci. Eng.* **3** 201
- [12] Lindemann F A 1910 *Phys. Z* **11** 609
- [13] Couchman R R 1979 *Phil. Mag. A* **40** 637
- [14] Berry R S 1990 *Sci. Am.* **263** 50
- [15] Broughton J Q and Gilmer G H 1986 *Phys. Rev. Lett.* **56** 2692